American Mineralogist, Volume 97, pages 1670–1675, 2012

Simultaneous sound velocity and density measurements of NaCl at high temperatures and pressures: Application as a primary pressure standard

Masanori Matsui,[1,*] Yuji Higo,[2] Yoshihiro Okamoto,[1] Tetsuo Irifune,[3] and Ken-Ichi Funakoshi[2]

[1]School of Science, University of Hyogo, Kouto, Kamigori, Hyogo 678-1297, Japan
[2]Japan Synchrotron Radiation Research Institute, Kouto, Hyogo 679-5198, Japan
[3]Geodynamic Research Center, Ehime University, Bunkyo-cho, Matsuyama 790-8577, Japan

Abstract

The elastic compressional (P) and shear (S) wave velocities in NaCl were measured up to 12 GPa at 300 K, and up to 8 GPa at 473 and 673 K, by combining ultrasonic interferometry, in situ synchrotron X-ray diffraction, and X-ray radiographic techniques in a large-volume Kawai-type multi-anvil apparatus. The simultaneously measured sound velocity and density data at 300 K and high pressures up to 12 GPa were corrected to transform the adiabatic values to isothermal values and then used to estimate the 300 K equation of state (EOS) by a least-squares fit to the fourth-order Birch-Murnaghan finite strain equation, without pressure data. For a fixed isothermal bulk modulus K_{T0} of 23.7 GPa at 0 GPa and 300 K, we obtained the first and the second pressure derivatives of K_{T0}, $K'_{T0} = 5.14 \pm 0.05$ and $K''_{T0} = -0.392 \pm 0.021$ GPa^{-1}, respectively. A high-temperature and high-pressure EOS of NaCl was then developed using the Mie-Grüneisen relation and the Debye thermal model. To accomplish this, the simultaneously measured sound velocities and densities up to 8 GPa at both 473 and 673 K, as well as previously reported volume thermal expansion data of NaCl at 0 GPa were included in the fit. This resulted in a q parameter of 0.96, while holding the Grüneisen parameter and the Debye temperature, both at 0 GPa and 300 K, fixed at 1.56 and 279 K, respectively. Our EOS model accurately modeled not only the present measured K_T data at pressures up to 12 GPa and temperatures between 300 and 673 K, but also the previously reported volume thermal expansion and the temperature dependence of K_T, both at 0 GPa. The new temperature-pressure-volume EOS for NaCl, presented here, provides a pressure-independent primary pressure standard at high temperatures and high pressures.

Keywords: Sound velocity, equation of state, NaCl, pressure standard, high pressure, high temperature, synchrotron X-ray

Introduction

The temperature-pressure-volume (*T-P-V*) equation of state (EOS) of the B1 phase of NaCl developed by Decker (1971) has been widely used as a practical pressure scale at temperatures and pressures up to 1200 K and 25 GPa. Brown (1999) reevaluated the *T-P-V* EOS based on a Mie-Grüneisen-Debye-type treatment with updated measured thermal and thermoelastic data for NaCl, and found that the new model for the *T-P-V* EOS for NaCl agrees well with that developed by Decker (1971). The two EOS values differ by <0.5 GPa over wide *T* and *P* ranges up to 1200 K and 25 GPa. Matsui (2009) performed molecular dynamics (MD) simulations using accurate empirical interatomic potentials to obtain a *T-P-V* EOS for NaCl and found that the MD EOS also agrees well with the EOS developed by Decker (1971). The two EOS values differ by at most 1 GPa up to 1200 K and 30 GPa.

The NaCl EOS was called into question, however, by Li et al., who directly determined the pressure by simultaneously measuring the sound velocities and densities of Mg_2SiO_4 wadsleyite (Li et al. 2005) and MgO (Li et al. 2006) at 300 K and high pressures. The samples examined experimentally by Li et al. (wadsleyite or MgO) were surrounded by a mixture of NaCl and boron nitride (BN) (NaCl:BN = 10:1 by weight), and the X-ray diffraction patterns from both the sample and the NaCl were collected to obtain the respective densities simultaneously at given pressures. The directly determined "absolute" pressure from the wadsleyite sample at 20 GPa and 300 K was 12(1)% (2.3 GPa) higher than the pressure in NaCl predicted by the Decker EOS.

The *T-P-V* EOS of NaCl is important, and many high-pressure studies rely on the pressures estimated based on the EOS of NaCl. Direct pressure measurements of NaCl at 300 K and high temperatures are required for such studies. To this end, Mueller et al. (2003) simultaneously measured the elastic wave velocities and static volume compression at pressures up to 8 GPa and 300 K. Their measurement technique involved measuring the sample length at high pressures by scanning the sample and monitoring changes in the sample X-ray diffraction intensity, which can yield significant errors in the estimated sample lengths and in the calculated sound velocities.

Following the technique described by Decremps et al. (2000) and Li et al. (2004), we recently developed (Higo et al. 2008, 2009) a sound-velocity measurement system at high pressures and high temperatures by combining ultrasonic interferometry, in situ synchrotron X-ray diffraction, and X-ray radiographic

* E-mail: m.matsui@sci.u-hyogo.ac.jp

0003-004X/12/0010–1670$05.00/DOI: http://dx.doi.org/10.2138/am.2012.4136

techniques in a large-volume Kawai-type multi-anvil apparatus. Using this technique, we performed accurate simultaneous measurements of the sound velocities and densities of NaCl at high pressures, up to 12 GPa and 300 K, and up to 8 GPa at both 473 and 673 K. The measured data at 300 K were used to obtain a 300 K volume compression curve for NaCl based on the fourth-order Birch-Murnaghan finite strain equation, without relying on a pressure scale. The measured data at 473 and 673 K were then used to estimate the thermal pressures at high temperatures and high pressures, based on the Mie-Grüneisen relation and the Debye thermal model, again without relying on a pressure scale. A *T-P-V* EOS was developed for NaCl to provide a primary pressure standard, which is applicable to static experiments at high temperatures and high pressures up to 1200 K and 25–30 GPa.

Experiments

Ultrasonic and synchrotron X-ray diffraction experiments at high temperatures and high pressures were performed using a Kawai-type multi-anvil (KMA) apparatus SPEED1500 at SPring-8 (beamline BL04B1). The experimental setup has been described in detail (Higo et al. 2008, 2009). The NaCl powders were ground and pressed into pellets 2.0 mm in diameter and 1.3 mm in length at 400–420 K to permit full dehydration. The NaCl samples were inserted into a Si_3N_4 capsule to perform stable ultrasonic measurements of soft materials, such as NaCl, at high temperatures and high pressures. Tungsten carbide (WC) anvils with an edge length of 26.0 mm and a truncated corner of 7.0 mm were used for the experiments. A schematic illustration of the cell assemblage is shown in Figure 1a. The acoustic travel times through the sample were determined using a pulse echo overlap method developed by Li et al. (2002, 2004). Dual-mode $LiNbO_3$ transducers (10° rotated Y-cut) were used to generate and receive both P and S sound waves. A transducer was positioned on the truncated outside corner of one of the WC anvils. The travel times were measured based on the reflections from the WC cube, the polycrystalline ZrO_2 buffer rod, the sample, and the Si_3N_4 capsule. Both ends of the buffer rod, the sample, and the top of the Si_3N_4 capsule were polished carefully using diamond paste to prevent unnecessary scattering of the sound waves. The sample was heated in a cylindrical graphite tube, and the temperatures were measured using a $W_{97}Re_3$-$W_{75}Re_{25}$ thermocouple. The temperature gradient within the sample was shown previously to be <5% (Higo et al. 2008, 2009).

The X-ray beam was directed toward the sample through a MgO window, a graphite heater, a BN sleeve, and a Si_3N_4 capsule through a small gap in the WC anvils. BN was loaded into the cell to provide a more hydrostatic environment. A solid-state germanium detector was used for energy-dispersive X-ray diffraction at a fixed 2θ angle of about 6°. Thin gold foils (2.5 μm thick) were positioned at both ends of the sample to improve mechanical coupling of the sound waves and to more clearly observe the X-ray images of sample ends. The sound velocities were obtained from the travel times and the sample length, that is, the distance between the gold foils determined by X-ray radiographic imaging using the CCD camera (Fig. 1b). The errors in the sample length were <1% using this technique. Semi-sintered ZrO_2 was used as a pressure medium to press and heat the sample efficiently. The correction in the travel time for the effects of the bond due to gold foils (Niesler and Jackson 1989) was estimated to be insignificant, and thus neglected in this study.

Experimental data were recorded after heating the sample to 873 K under a fixed press load to minimize non-hydrostatic components due to local deviatoric stresses. Heating to 873 K reduced the diffraction peak widths substantially, as shown in Figure 2. The NaCl cubic lattice parameters at high temperatures and high pressures were obtained using 6–8 reflections with indices (2 0 0), (2 2 0), (2 2 2), (4 0 0), (3 3 1), (4 2 0), or (4 2 2) (see Fig. 2). We successfully obtained 7 high-quality data at 300 K and pressures up to 12 GPa, and two data at each of 473 and 673 K and pressures of 7–8 GPa, as shown in Table 1.

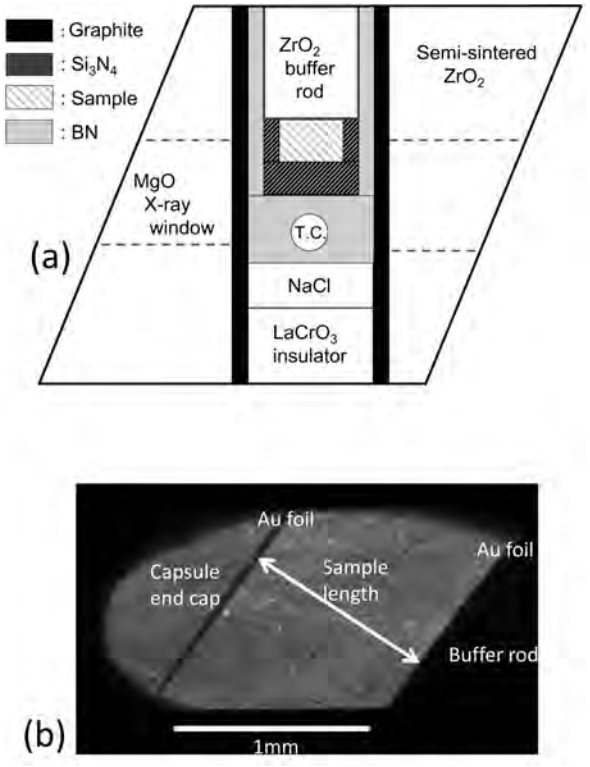

Figure 1. (**a**) A cross-section image of the furnace cell assembly used in this work: graphite heater, Si_3N_4 capsule, sample (NaCl), BN sleeve, and thermocouple (T.C.). (**b**) An X-ray radiographic image used to measure the sample length.

Results and Discussion

The measured P- and S-wave velocities, v_P and v_S, respectively, along with density ρ, can be used to express the adiabatic bulk modulus K_S as: $K_S = (v_P^2 - 4/3\ v_S^2) \times \rho$. K_S can be converted to the isothermal bulk modulus K_T using the relation

$$K_T = K_S/(1 + \alpha\gamma T) \quad (1)$$

where α and γ are the volume thermal expansivity and the Grüneisen constant, respectively. Here we adopted the α and γ values as a function of ρ, based on the EOS's for NaCl proposed by Matsui (2009) and Brown (1999), respectively. The error

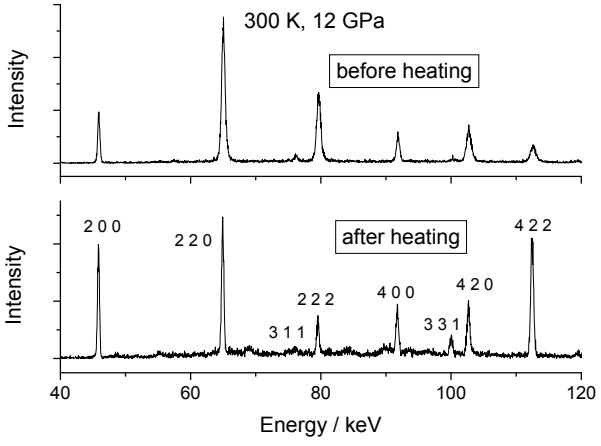

Figure 2. Measured diffraction pattern for NaCl at 300 K and 12 GPa, before and after heating the sample to 873 K.

TABLE 1. Observed relative volume (V/V_0)*, density (ρ), P- and S-wave velocities (v_P, v_S), and the adiabatic and isothermal bulk moduli (K_S, K_T) at 300, 473, and 673 K, compared with the calculated isothermal bulk modulus [K_T(calc)] and the "absolute" pressure [P(calc)] based on the EOS model given in Table 2

T (K)	V/V_0	ρ (g/cm³)	v_P (km/s)	v_S (km/s)	K_S (GPa)	K_T (GPa)	K_T(calc) (GPa)	P(calc) (GPa)
300	0.7669(3)	2.821(1)	6.08(5)	2.848(26)	73.74	73.0(18)	73.2	12.04
300	0.7702(3)	2.809(1)	6.06(5)	2.845(29)	72.88	72.2(19)	72.1	11.73
300	0.7742(4)	2.794(1)	6.03(5)	2.846(26)	71.42	70.7(18)	70.7	11.35
300	0.7860(5)	2.752(2)	5.95(6)	2.841(29)	67.78	67.0(19)	66.9	10.31
300	0.8115(3)	2.666(1)	5.70(6)	2.786(32)	59.12	58.3(20)	59.4	8.30
300	0.8291(6)	2.609(2)	5.61(4)	2.776(20)	55.30	54.5(12)	54.7	7.07
300	0.8355(2)	2.589(1)	5.58(4)	2.772(17)	54.00	53.1(10)	53.0	6.66
473	0.8310(6)	2.603(2)	5.58(3)	2.726(13)	55.37	53.8(8)	54.1	7.43
473	0.8358(3)	2.589(1)	5.56(3)	2.725(16)	54.29	52.7(9)	52.9	7.12
673	0.8340(3)	2.594(1)	5.57(4)	2.675(19)	55.59	53.4(11)	53.4	7.81
673	0.8379(3)	2.582(1)	5.54(3)	2.673(13)	54.51	52.3(8)	52.4	7.56

* V_0 = 179.425 Å³ (JCPDS card 05-0628).

introduced from the α and γ values is insignificant because the correction factors for the conversion of K_S to K_T, $\alpha\gamma T$, are <2% for the data at 300 K and high pressures, and 3–4% for the data at both 473 and 673 K and high pressures, as listed in Table 1.

P- and S-wave velocities at 300 K

Figures 3a and 3b shows the measured P- and S-wave velocities as a function of the density, together with previous results for comparison. The v_P and v_S values at 300 K and 0 GPa were taken to be 4.55 ± 0.01 and 2.610 ± 0.003 km/s, respectively, using the Voigt-Reuss-Hill average obtained from the elasticity data reported in Chang (1965), Slagle and McKinstry (1967), Spetzler et al. (1972), and Yamamoto et al. (1987). The 300 K v_P data at high pressures and the 0 GPa value (4.55 km/s) taken from previous reports displayed a linear dependence on density (see Fig. 3a), known as Birch's law (Birch 1960), with a slope of $dv_P/d\rho = 2.35(1)$ km s^{-1} (g/cm^3)$^{-1}$. Campbell and Heinz (1992) used Brillouin scattering and diamond-anvil cell experiments to measure the v_P velocities in NaCl at 300 K and pressures up to 17 GPa. Their data fit well to Birch's law, with $dv_P/d\rho = 2.616(35)$ km s^{-1} (g/cm^3)$^{-1}$. Frankel et al. (1976) used ultrasonic interferometry techniques with a Bridgeman anvil device and reported the v_P and v_S velocities in NaCl at 300 K and pressures of 2.5–27 GPa. They estimated the sample thickness during each measurement based on the EOS for NaCl, as proposed by Decker (1971). Their data showed a linear relationship between v_P and ρ, and lie between the data by Campbell and Heinz (1992) and our data sets, as shown in Figure 3a.

The 300 K v_S data measured here at high pressures together with v_S = 2.61 km/s at 0 GPa determined from previous investigations also showed that v_S increased linearly with density, within the measured error, with a slope of $dv_S/d\rho = 0.370(5)$ km s^{-1} (g/cm^3)$^{-1}$, as shown in Figure 3b. The v_S values reported by Frankel et al. (1976) or Campbell and Heinz (1992) deviated from linearity (see Fig. 3b). It should be noted, however, that the scale spanned by v_P plotted in Figure 3a is more than four times the scale spanned by v_S shown in Figure 3b. The discrepancies between the data reported in Frankel et al. and our own data may be due in part to differences in the pressure calibration technique. Frankel et al. estimated measured pressures based on the observation of resistometric changes of standard materials,

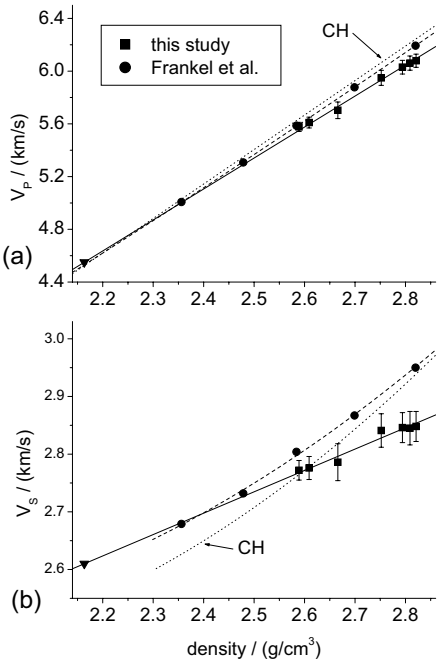

FIGURE 3. Measured P- and S-wave velocities, v_P (**a**) and v_S (**b**), respectively (squares, solid lines) as a function of the density ρ at room temperature. Also shown are the values reported previously: Frankel et al. (1976) (circles, broken lines) and Campbell and Heinz (1992) (CH, dotted lines). The values at 0 GPa (ρ = 2.164 g/cm^3, inverted triangles) are from Chang (1965), Slagle and McKinstry (1967), and Spetzler et al. (1972). Note that the scale of the v_P values given in **a** is more than four times the scale of the v_S values given in **b**.

and found the pressure error to be <15% up to 29 GPa (Frankel et al. 1976). We note that the values of v_S reported by Campbell and Heinz (1992) were estimated indirectly by combining the measured values of v_P with the EOS proposed by Birch (1978), based on the relation $K_S/\rho = v_P^2 - 4/3\ v_S^2$.

300 K equation of state

P and K_T at constant temperature can be expressed using the fourth-order Birch-Murnaghan finite strain equation (Birch 1986),

$$P = 3fK_{T0}(1 + 2f)^{5/2}(1 + af + bf^2) \quad (2)$$

$$K_T = -V(\partial P/\partial V)_T = K_{T0}(1 + 2f)^{5/2}[1 + (7 + 2a)f + (9a + 3b)f^2 + 11bf^3] \quad (3)$$

in which f is the Eulerian strain defined by

$$V/V_0 = (1 + 2f)^{-3/2} \quad (4)$$

and

$$a = (3/2)(K'_{T0} - 4) \quad (5)$$

$$6b = 9K_{T0}K''_{T0} + 9(K'_{T0})^2 - 63K'_{T0} + 143. \quad (6)$$

The subscript zero indicates values at $P = 0$ and 300 K, and K'_{T0} and K''_{T0} are the first and second pressure derivatives of K_{T0}. γ_0 was estimated, using the relation $\gamma = \alpha V K_S / C_P$ at 300 K and 0 GPa, to be 1.56 based on the values $\alpha_0 = 1.175 \times 10^{-4}$ K^{-1}, reported in Enck and Dommel (1965), $V_0 = 179.425$ Å^3 from JCPDS (card 05-0628), $K_{S0} = 25.0$ GPa from Chang (1965), Slagle and McKinstry (1967), and Decker (1971), and the constant-pressure heat capacity $C_{P0} = 8.68$ J/(gK) from Stull and Prophet (1971). K_{T0} was fixed at 23.7 GPa, based on the value of $K_{S0} = 25.0$ GPa given above, $\alpha_0\gamma_0 T = 0.055$, and the two key EOS parameters, K'_{T0} and K''_{T0}, were determined by fitting Equation 3 to the measured values of K_T as a function of f data at 300 K, as given in Table 1, by the method of least squares. One data point with $\rho = 2.666$ g/cm^3 ($f = 0.0747$ in Fig. 4) was removed from the data set during final fitting, as this data deviated substantially from a single K_T – f curve, as shown in Figure 4. The K'_{T0} and K''_{T0} values obtained are given in Table 2. The "absolute" pressures calculated at 300 K using Equation 2 based on the present EOS model are given in Table 1.

The measured v_P and v_S velocities (in km/s) at 300 K and pressures up to 12.04 GPa (Table 1) are given in the following quadratic polynomials in "absolute" pressure (in GPa): $v_P = 4.55 + 0.180(5) \times P - 0.0044(4) \times P^2$, and $v_S = 2.61 + 0.028(2) \times P - 0.0007(2) \times P^2$, holding $(v_P)_0$ and $(v_S)_0$ fixed at 4.55 and 2.61 km/s, respectively, from the elasticity data reported in Chang (1965), Slagle and McKinstry (1967), and Spetzler et al. (1972). Table 3 shows a comparison of the pressure derivatives of v_P and v_S at 300 K and 0 GPa between our measured values and previously reported ones based on ultrasonic measurements gathered from powder samples by Frankel et al. (1976), Morris et al. (1976), and Mueller et al. (2003) at pressures up to 27, 9, and 8 GPa, respectively, Brillouin scattering experiments performed by Campbell and Heinz (1992) at pressures up to 17 GPa, and the ultrasonic measurements of Spetzler et al. (1972), performed using single crystals at pressures between 0 and 0.8 GPa and temperatures between 300 and 800 K. The v_P and v_S values of Spetzler et al. are estimated using the Voigt-Reuss-Hill average based on their reported elastic constants. The pressure derivatives of v_P or v_S reported here differ from those reported previously, partly due to uncertainties in the sample length. The sample length in previous studies were estimated indirectly based on the isothermal EOS's, thermodynamic properties (Frankel et al. 1976; Morris et al. 1976; Spetzler et al. 1972), or the scanned X-ray diffraction intensities (Mueller et al. 2003). Here, the sample lengths were measured directly and accurately at high temperatures and high pressures using X-ray radiographic techniques, as shown in Figure 1b. The discrepancies in the pressure derivatives may also have arisen from the effects of nonhydrostatic stresses in the samples at high pressures because all previous measurements, except for those performed by Spetzler et al. (1972), were performed at 300 K without sample annealing. On the other hand, our data were obtained using a sample annealed at 873 K, as already stated (see Fig. 2). We further note that the discrepancies in the pressure derivatives could result from errors in the pressure estimates or from the different pressure ranges used for measurements. The high-pressure derivatives of both v_P and v_S, reported by Spetzler et al. (1972), may be due to an overestimation of the effective pressure at lower pressures, as suggested by Birch (1978).

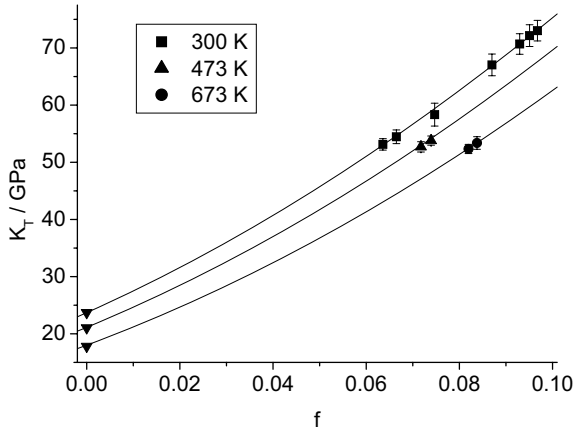

FIGURE 4. Measured isothermal bulk moduli K_T as a function of the Eulerian strain f at 300 K (squares), 473 K (triangles), and 673 K (circles), together with the calculated values (solid lines) based on the present EOS model given in Table 2, for comparison. The values observed at $f = 0$ (inverted triangles) are from Chang (1965), Slagle and McKinstry (1967), and Decker (1971) for the data at 300 K, and from interpolation using the data reported in Spetzler et al. (1972) for the data at 473 and 673 K.

TABLE 2. The optimized EOS parameters for NaCl, in comparison with the values reported previously

Parameters	This study*	Decker†	Birch‡
K_{T0} (GPa)	23.7(fixed)	23.70(1)	23.88
K'_{T0}	5.14(5)	4.91(1)	5.20
K''_{T0} (GPa^{-1})	–0.392(21)	–0.267(2)	–0.41
Θ_0 (K)	279(fixed)	279	–
γ_0	1.56(fixed)	1.59	1.62(2)
q	0.96	0.93	1

* See the text for the fixed values.
† For Decker (1971), the K_{T0}, K'_{T0}, K''_{T0} values were obtained using Equation 2 by a least-squares fitting based on their reported P-V relations at room temperature.
‡ From Birch (1986). The value of q is provided in the text.

High-temperature and high-pressure equation of state

The T-P-V EOS is often expressed using the Mie-Grüneisen-Debye type treatment, as described previously (Matsui et al. 2009, 2012), in which the pressure at a fixed V is expressed as a function of T as

TABLE 3. A comparison of the P- and S-wave velocities (v_P and v_S, respectively, in km/s), and their pressure derivatives [km/(s·GPa)] at 300 K and 0 GPa, measured in this study, with those measured previously

	$(v_P)_0$	$(dv_P/dP)_0$	$(v_S)_0$	$(dv_S/dP)_0$	P_{max}§
This study	4.55(fixed)*	0.180(5)	2.61(fixed)*	0.028(2)	12
Frankel et al. (1976)†	[4.596(5)]	[0.174(2)]	[2.591(7)]	[0.035(2)]	27
Morris et al. (1976)	4.56	0.247	2.63	0.063	9
Campbell and Heinz (1992)	4.525	0.237	2.54	0.035	17
Mueller et al. (2003)	4.56	0.14	2.60	0.029	8
Spetzler et al. (1972)‡	4.556	0.294	2.612	0.106	0.8

* See the text for the fixed values.
† Extrapolated using a quadratic polynomial fit to the v_P-P or v_S-P data reported by Frankel et al. (1976) between 2.5 and 12 GPa.
‡ Voigt-Reuss-Hill values averaged from the elastic constants reported in Spetzler et al. (1972), after Birch (1978).
§ Maximum measured pressure, in GPa.

$$P(V,T) = P(V, 300\ \mathrm{K}) + P_{\mathrm{TH}}(V,T). \quad (7)$$

In this equation, $P(V, 300\ \mathrm{K})$ is the pressure at 300 K (as expressed by Eq. 2), and $P_{\mathrm{TH}}(V,T)$ is the thermal pressure, caused by heating from 300 K to T at constant V. $P_{\mathrm{TH}}(V,T)$ is obtained from the Mie-Grüneisen equation, as

$$P_{\mathrm{TH}}(V,T) = (\gamma/V)\,[E_{\mathrm{TH}}(V,T) - E_{\mathrm{TH}}(V,300\ \mathrm{K})] \quad (8)$$

where $E_{\mathrm{TH}}(V,T)$ is the internal energy at V and T, and γ is assumed to be a function of volume only, independent of temperature, approximated as,

$$\gamma = \gamma_0\,(V/V_0)^q \quad (9)$$

in which q is a fitting constant. $E_{\mathrm{TH}}(V,T)$ can be calculated using the Debye model,

$$E_{\mathrm{TH}}(V,T) = [9nRT/(\Theta/T)^3] \int_0^{\Theta/T} z^3/(e^z - 1)\,dz\,, \quad (10)$$

where $n = 2$ for NaCl, R is the gas constant, and Θ is the Debye temperature, such that Θ is written as

$$\Theta = \Theta_0 \exp[(\gamma_0 - \gamma)/q] \quad (11)$$

where Θ_0 is the value at 300 K and 0 GPa. Thus, in addition to the values of K_{T0}, K'_{T0}, K''_{T0}, and γ_0 given in Table 2, the parameters q and Θ_0 are required to fully describe the *T*-*P*-*V* EOS for NaCl. Of these parameters, Θ_0 was fixed at 279 K, as reported by Decker (1971). Similar values of $\Theta_0 = 276$ and 308 K were reported by Brown (1999) and Yamamoto et al. (1987), respectively. The remaining parameter q was derived here to reproduce not only the measured K_{T} values at both 473 and 673 K and pressures of 7–8 GPa, as given in Table 1, but also the observed volume thermal expansion at 0 GPa reported by Enck and Dommel (1965). The optimized EOS parameters are listed in Table 2, together with those reported in previous studies for comparison. The "absolute" pressures at 473 and 673 K, calculated using Equation 7 with the present EOS model, are given in Table 1.

The K_{T} values calculated at 300, 473, and 673 K and pressures between 6.6 and 12.1 GPa, based on our EOS model, as listed in Table 2, agree with the measured values, within measured errors, as shown in Table 1 and Figure 4. The calculated volume thermal expansion at 0 GPa also agrees well with the measured data reported by Enck and Dommel (1965), with the calculated and measured V/V_0 values differing by <0.1% at temperatures between 300 and 800 K. This agreement may be expected because the q parameter in the present EOS model was developed to reproduce the observed volume thermal expansion, as well as the present measured K_{T} values at 473 and 673 K, as described above. The ambient-pressure volumes at $T = 473$ and 673 K are calculated to be $V(T,0)/V_0 = 1.0219$ and 1.0521, respectively, using the present EOS model (Table 2). We note the f values for the data at 473 and 673 K and high pressures P, given in Figure 4, are estimated based on these $v(T,0)$ values using the equation: $V(T,P)/V(T,0) = (1 + 2f)^{-3/2}$, instead of Equation 4 at 300 K.

The ambient-pressure K_{T} values for several isotherms were calculated using the fourth-order Birch-Murnaghan EOS (Eq. 2) at constant T and the EOS parameters given in Table 2. The present model successfully and accurately reproduces the measured temperature dependence of the ambient-pressure K_{T}, as shown in Figure 5. Birch (1986) developed a *T*-*P*-*V* EOS for NaCl up to temperatures of 773 K and 30 GPa based on previously reported ultrasonic, static volumetric, and shock compression data, in which the room-temperature EOS is expressed using the fourth-order Birch-Murnaghan Equation 2, and the thermal pressure is estimated by assuming that the $(\gamma/V)C_V$ [$=(\partial P/\partial T)_V$] is independent of both P and T (C_V, constant-volume heat capacity). A constant value of $(\gamma/V)C_V$ indicates that $q = 1$ in the Birch's EOS in the high-temperature classical limit. As shown in Figure 5, the temperature dependence of the ambient-pressure K_{T} described by Birch (1986) also accurately reproduces the experimental data.

We note that a similar Mie-Grüneisen-Debye type analysis using the third-order (instead of the fourth-order) Birch-Murnaghan equation was also successful in reproducing the present measured K_{T}-f relation at each temperature given in Figure 4 within the measured errors. However, this EOS model based on the third-order Birch-Murnaghan equation gave a smaller slope of dK_{T}/dT than that measured experimentally (Spetzler et al. 1972; Yamamoto et al. 1987) or that predicted by the present fourth-order EOS model, given in Figure 5.

Table 2 shows a comparison between our EOS model and the models proposed in previous studies. The values of K_{T0}, K'_{T0}, and K''_{T0} from Decker (1971) were adjusted here by fitting his reported *P*-*V* data at room temperature to Equation 2 using the least-squares method. The EOS parameters optimized in this study agree well with those described by Decker (1971) and Birch (1986), as shown in Table 2, considering that K_{T0} and K'_{T0} are strongly correlated, as are K'_{T0} and K''_{T0}. The present EOS is in excellent agreement with Birch's EOS, and the differences between the two (i.e., Birch's minus ours) are within 0.23 GPa over the temperature and pressure ranges up to 773 K and 25 GPa.

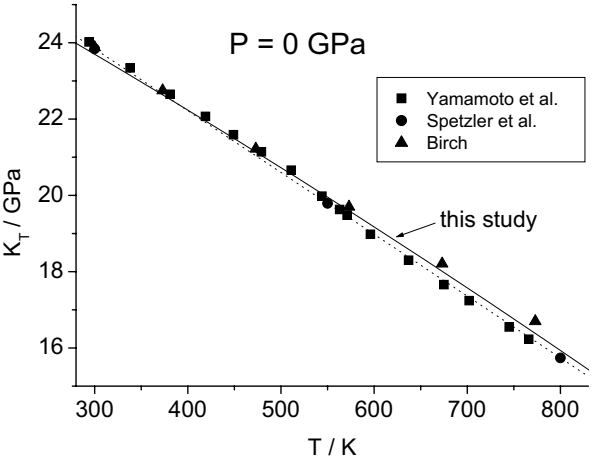

FIGURE 5. Observed and calculated temperature dependence of the isothermal bulk modulus K_{T} at 0 GPa. The observed data were reported in Yamamoto et al. (1987) (squares) and Spetzler et al. (1972) (circles and dotted line), and the calculated results were obtained using the present EOS model as given in Table 2 (this study, solid line), and from the EOS model described by Birch (1986) (triangles).

TABLE 4. Pressures (GPa) calculated at selected volumes and temperatures

V/V_0	300 K	500 K	700 K	900 K	1200 K
1.0	0.0(0.0)*	0.56(0.58)	1.13(1.16)	1.70(1.74)	2.57(2.62)
0.95	1.39(1.38)	1.95(1.96)	2.52(2.54)	3.09(3.12)	3.95(4.00)
0.90	3.26(3.24)	3.82(3.81)	4.39(4.39)	4.96(4.98)	5.82(5.86)
0.85	5.78(5.74)	6.33(6.31)	6.90(6.89)	7.48(7.48)	8.34(8.37)
0.80	9.17(9.13)	9.72(9.70)	10.29(10.28)	10.87(10.87)	11.73(11.76)
0.75	13.73(13.76)	14.28(14.33)	14.85(14.91)	15.43(15.50)	16.29(16.39)
0.70	19.88(20.15)	20.42(20.71)	20.99(21.30)	21.57(21.89)	22.44(22.78)
0.65†	28.16(29.07)	28.71(29.63)	29.27(30.22)	29.85(30.81)	30.72(31.71)

* The pressure values in parentheses are from Decker (1971).
† Note that NaCl transforms to the CsCl structure at 29.3 GPa and 300 K, and at 24.2 GPa and 1200 K (Nishiyama et al. 2003).

Finally, the calculated pressures as functions of temperature and volume are presented in Table 4 together with the values given by Decker (1971). The present and Decker's EOS's agree within 0.34 GPa over the compression and temperature ranges up to $V/V_0 = 0.70$ and 1200 K, and agree within 1 GPa at a compression of $V/V_0 = 0.65$ and temperatures between 300 and 1200 K, as can be seen in Table 4.

ACKNOWLEDGMENTS

The authors thank Donald Isaak, Ian Jackson, and Jennifer Kung (Associate Editor) for their constructive comments and helpful suggestions. The experiments were conducted using the beamline BL04B1 at SPring-8 (Proposal Nos. 2008B2210, 2009A1951, and 2009B2125). This work was supported by a Grant-in-Aid for Scientific Research from The Ministry of Education, Culture, Sports, Science and Technology (No. 24540520 to M.M.).

REFERENCES CITED

Birch, F. (1960) The velocity of compressional waves in rocks to 10 kilobars, Part 1. Journal of Geophysical Research, 65, 1083–1102.
——— (1978) Finite strain isotherm and velocities for single-crystal and polycrystalline NaCl at high pressures and 300° K. Journal of Geophysical Research, 83, 1257–1268.
——— (1986) Equation of state and thermodynamic parameters of NaCl to 300 kbar in the high-temperature domain. Journal of Geophysical Research, 91, 4949–4954.
Brown, J.M. (1999) The NaCl pressure standard. Journal of Applied Physics, 86, 5801–5808.
Campbell, A.J. and Heinz, D.L. (1992) A high-pressure test of Birch's law. Science, 257, 66–68.
Chang, Z.-P. (1965) Third-order elastic constants of NaCl and KCl single crystals. Physical Review, 140, A1788–A1799.
Decker, D.L. (1971) High-pressure equation of state for NaCl, KCl, and CsCl. Journal of Applied Physics, 42, 3239–3244.
Decremps, F., Zhang, J., and Liebermann, R.C. (2000) New phase boundary and high-pressure thermoelasticity of ZnO. Europhysics Letters, 51, 268–274.
Enck, F.D. and Dommel, J.G. (1965) Behavior of the thermal expansion of NaCl at elevated temperatures. Journal of Applied Physics, 36, 839–844.
Frankel, J., Rich, F.J., and Homan, C.G. (1976) Acoustic velocities in polycrystalline NaCl at 300° K measured at static pressures from 25 to 270 kbar. Journal of Geophysical Research, 81, 6357–6363.
Higo, Y., Inoue, T., Irifune, T., Funakoshi, K., and Li, B. (2008) Elastic wave velocities of $(Mg_{0.91}Fe_{0.09})_2SiO_4$ ringwoodite under *P-T* conditions of the mantle transition region. Physics of the Earth and Planetary Interiors, 166, 167–174.
Higo, Y., Kono, Y., Inoue, T., Irifune, T., and Funakoshi, K. (2009) A system for measuring elastic wave velocity under high pressure and high temperature using a combination of ultrasonic measurement and the multi-anvil apparatus at SPring-8. Journal of Synchrotron Radiation, 16, 762–768.
Li, B., Chen, K., Kung, J., and Liebermann, R.C., and Weidner, D.J. (2002) Sound velocity measurement using transfer function method. Journal of Physics: Condensed Matter, 14, 11337–11342.
Li, B., Kung, J., and Liebermann, R.C. (2004) Modern techniques in measuring elasticity of Earth materials at high pressure and high temperature using ultrasonic interferometry in conjunction with synchrotron X-radiation in multi-anvil apparatus. Physics of the Earth and Planetary Interiors, 143–144, 559–574.
Li, B., Kung, J., Uchida, T., Wang, Y. (2005) Pressure calibration to 20 GPa by simultaneous use of ultrasonic and X-ray techniques. Journal of Applied Physics, 98, 013521.
Li, B., Woody, K., and Kung, J. (2006) Elasticity of MgO to 11 GPa with an independent absolute pressure scale: Implications for pressure calibration. Journal of Geophysical Research, 111, B11206, doi:10.1029/2005JB004251.
Matsui, M. (2009) Temperature-pressure-volume equation of state of the B1 phase of sodium chloride. Physics of the Earth and Planetary Interiors, 174, 93–97.
Matsui, M., Ito, E., Katsura, T., Yamazaki, D., Yoshino, T., Yokoyama, A., and Funakoshi, K. (2009) The temperature-pressure-volume equation of state of platinum. Journal of Applied Physics, 105, 013505.
Matsui, M., Ito, E., Yamazaki, D., Yoshino, T., Guo, X., Shan, S., Hogo, Y., and Funakoshi, K. (2012) Static compression of $(Mg_{0.83},Fe_{0.17})O$ and $(Mg_{0.75},Fe_{0.25})O$ ferropericlase up to 58 GPa at 300, 700, and 1100 K. American Mineralogist, 97, 176–183.
Morris, C.E., Jamieson, J.C., and Yarger, F.L. (1976) Ultrasonic measurements at elevated pressures (9 GPa) to determine Poison's ratio and other elastic moduli of NaCl and NaF. Journal of Applied Physics, 47, 3979–3986.
Mueller, H.J., Schilling, F.R., Lauterjung, J., and Lathe, C. (2003) A standard-free pressure calibration using simultaneous XRD and elastic property measurements in a multi-anvil device. European Journal of Mineralogy, 15, 865–873.
Niesler, H. and Jackson, I. (1989) Pressure derivatives of elastic wave velocities from ultrasonic interferometric measurements on jacketed polycrystals, Journal of the Acoustical Society of America, 86, 1573–1585.
Nishiyama, N., Katsura, T., Funakoshi, K., Kubo, A., Kubo, T., Tange, Y., Sueda, Y., and Yokoshi, S. (2003) Determination of the phase boundary between the B1 and B2 phases in NaCl by in situ X-ray diffraction, Physical Review B, 68, 134109.
Slagle, O.D. and McKinstry, H.A. (1967) Temperature dependence of the elastic constants of the alkali halides. I. NaCl, KCl, and KBr. Journal of Applied Physics, 38, 437–446.
Spetzler, H., Sammis, C.G., and O'Connell, R.J. (1972) Equation of state of NaCl: Ultrasonic measurements to 8 kbar and 800°C and static lattice theory. Journal of Physics and Chemistry of Solids, 33, 1727–1750.
Stull, D.R. and Prophet, H. (Eds) (1971) JANAF Thermochemical Tables (2nd ed.). U.S. Department of Commerce, National Bureau of Standards, Washington, D.C.
Yamamoto, S., Ohno, I., and Anderson, O.L. (1987) High temperature elasticity of sodium chloride. Journal of Physics and Chemistry of Solids, 48, 143–151.

MANUSCRIPT RECEIVED FEBRUARY 21, 2012
MANUSCRIPT ACCEPTED MAY 24, 2012
MANUSCRIPT HANDLED BY JENNIFER KUNG